



Effect of bias voltage on growth property of Cr-DLC film prepared by linear ion beam deposition technique

Wei Dai, He Zheng, Guosong Wu, Aiyang Wang*

Division of Surface Engineering and Remanufacturing, Ningbo Institute of Materials Technology and Engineering, Chinese Academy of Sciences, Ningbo, China

ARTICLE INFO

Article history:

Received 24 March 2010

Received in revised form

31 May 2010

Accepted 1 June 2010

Keywords:

Cr-DLC

Bias voltage

Atomic bond structure

Surface topography

Properties

ABSTRACT

Cr-containing diamond-like carbon films were deposited on silicon wafers by a combined linear ion beam and DC magnetron sputtering. The influence of the bias voltage on the growth rate, atomic bond structure, surface topography and mechanical properties of the films were investigated by SEM, XPS, Raman spectroscopy, AFM, and nano-indentation. It was shown that the chromium concentration of the films increased with negative bias voltage and that a carbide phase was detected in the as-deposited films. The surface topography of the films evolved from a rough surface with larger hillocks reducing to form a smoother flat surface as the bias voltage increased from 0 to -200 V. The highest hardness and elastic modulus were obtained at a bias voltage of about -50 V, while the maximum sp^3 bonding fraction was acquired at -100 V. It was suggested that the mechanical properties of the films not only depended on the sp^3 bonding fraction in the films but also correlated with the influence of Cr doping and ion bombardment.

© 2010 Elsevier Ltd. All rights reserved.

1. Introduction

Metal-containing amorphous hydrogenated carbon (Me-DLC) films have attracted significant attention owing to their excellent properties including high hardness, low friction coefficient and high wear-resistant. Additionally, they possess relatively low internal stress compared with pure DLC films [1–3]. Many techniques have been proposed for the deposition of Me-DLC films without substrate heating. Corbella and co-workers have successfully synthesized metal (W, Mo, Nb, Ti) containing DLC by reactive magnetron sputtering in a gas mixture of methane and argon [4]. Zhang et al. deposited Al-DLC films by a co-sputtering technique using a graphite target and an aluminum target [5]. Recently, Wang et al. used a hybrid ion beam deposition system, which consisted of an end-Hall ion beam and magnetron sputtering of a metal target to fabricate W-DLC films [6].

The microstructure and properties of the Me-DLC films depend critically on the deposition technique and process parameter [7,8]. It is well known that the energy of the carbon ion for DLC deposition determines the formation of sp^3 bonds and has an optimum value at about 100 eV per carbon atom [9]. In addition other ion bombardment effects, including sub-implantation, re-sputtering and etching during the film growth, strongly influence the

microstructure and surface topography of the DLC films [8–12]. Hence, the bias voltage employed to control the ion bombardment energy can be used to modify the microstructure, surface topography and mechanical properties of the coating.

In this paper, an anode-layer linear ion source (LIS) combined with a DC magnetron sputtering was used to prepare Cr-DLC films. This LIS can be scaled to any desired length and thus can produce ion beams for treating large-area samples [13]. During film deposition, a negative bias voltage was applied to the substrate. The growth rate, composition, surface topography and mechanical properties of the films were systematically investigated as a function of the bias voltage.

2. Experimental details

Fig. 1 shows the schematic diagram of the co-deposition system, which consists of a LIS and a magnetron sputtering source. The LIS with a cross-sectional area of $100\text{ mm} \times 380\text{ mm}$ faces to the substrate at an angle of 20° . The magnetron sputtering unit, equipped with a $100\text{ mm} \times 380\text{ mm}$ rectangular chromium target (99.99%), also faces to the substrate at an angle of 20° . The distance between the substrate and the LIS as well as the magnetron sputtering source was about 200 mm. A $525 \pm 15\ \mu\text{m}$ thick silicon wafer of size $20\text{ mm} \times 20\text{ mm}$ was used as the substrate. Another $285 \pm 5\ \mu\text{m}$ thick silicon wafer of size $3\text{ mm} \times 35\text{ mm}$ was also used as a substrate to accurately estimate the internal stress from the

* Corresponding author.

E-mail address: aywang@nimte.ac.cn (A.Y. Wang).

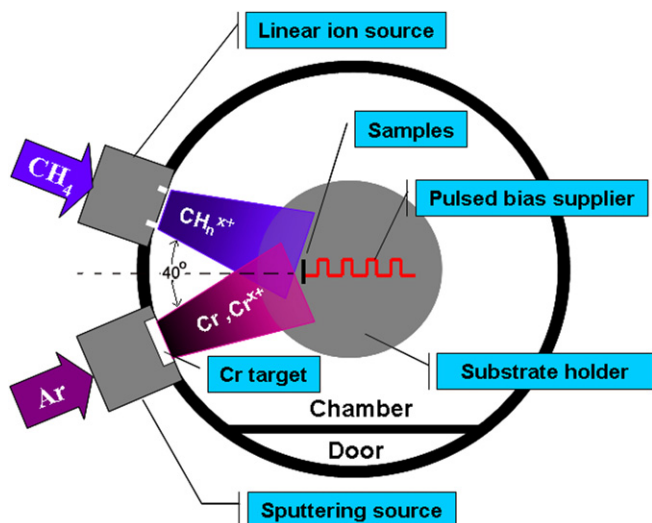


Fig. 1. Schematic diagram of the co-deposition system.

observed curvature of the film/substrate composite using the Stoney equation [14]. The curvature of the film/substrate was determined by a laser tester. All the wafers were cleaned ultrasonically in acetone for 10 min, and then dried in air. The chamber was first evacuated down to about 2.5×10^{-5} bar and purged by Ar^+ ions in the discharge which was run several times. Before deposition, the substrate was sputter-cleaned for 10 min using Ar^+ ions. Hydrocarbon gas (CH_4) with a gas flow of 25 sccm was introduced into the LIS to obtain the hydrocarbon ions, and Ar with a gas flow of 55 sccm was introduced into to the magnetron sputtering to sputter Cr. The deposition pressure was kept at about 4.4×10^{-3} bar. Typical values of the LIS voltage and current were 1200 ± 50 V and 0.2 A, respectively. The DC power (current model) supplied to the sputtering gun was about 950 W (2.5 A). The negative bias voltage varied from 0 (floating) to -200 V. No other parameters were changed between subsequent coatings.

The thickness of the as-deposited films was measured using a cross-sectional SEM (S-4800, Hitachi, Japan) and all film thicknesses were greater than 600 nm in general. The chemical composition of the films was analyzed using energy-dispersive X-ray spectroscopy (EDS). X-ray photoelectron spectroscopy (XPS, Axis ultradld, Japan) with Al (mono) $K\alpha$ irradiation at a pass energy of 160 eV was used to characterize the chemical bonds of the films. Raman spectroscopy

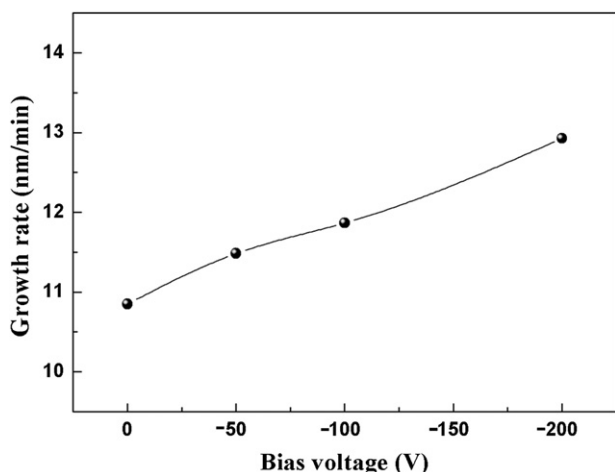


Fig. 2. Growth rate of the films as a function of the bias voltage.

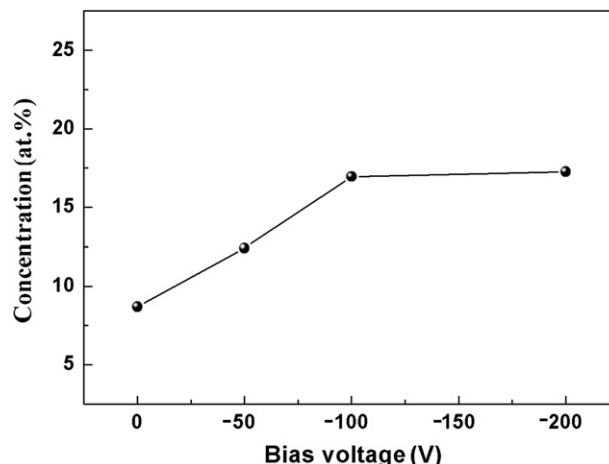


Fig. 3. Cr concentration of the films deposited at different bias voltage.

with an incident Ar^+ laser at a wavelength of 514.5 nm was used to evaluate the nature of the carbon atomic bonds in the films.

The surface topography and roughness of the films were observed using a Scanning Probe Microscope (SPM) (Dimension 3100 V, Veeco, US) and SEM. The surface wettability of the films was measured by a contact angle measurement system (OCA20, Data physics, Germany) in air at ambient temperature. Distilled water droplets of about $5 \mu\text{l}$ were carefully dropped onto the film surface. Mechanical properties were measured by the nano-indentation technique in a continuous stiffness measurement (CSM) mode with a maximum indentation depth of 500 nm. The characteristic hardness of the films was chosen as the value obtained at a depth where the measured value was not affected by the soft Si substrate.

3. Results and discussion

3.1. Growth and composition

The dependence of the average growth rate on the bias voltage is shown in Fig. 2. As the bias voltage increased from 0 (floating) to -200 V, the growth rate of the films increased slightly from about

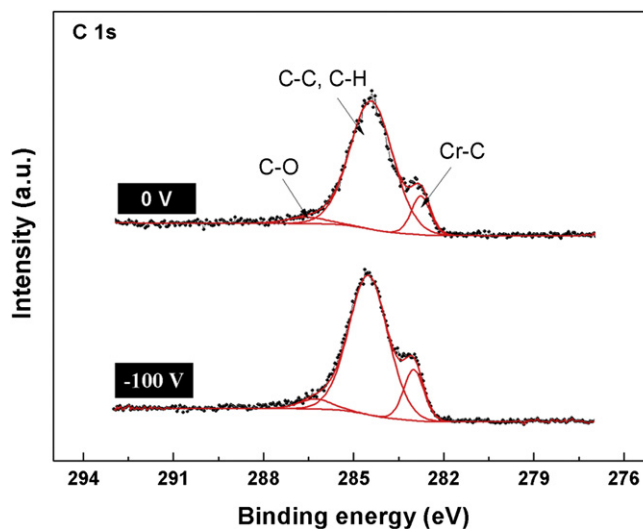


Fig. 4. Typical C 1s high-resolution XPS spectra of the films deposited with bias voltage of 0 V and -100 V.

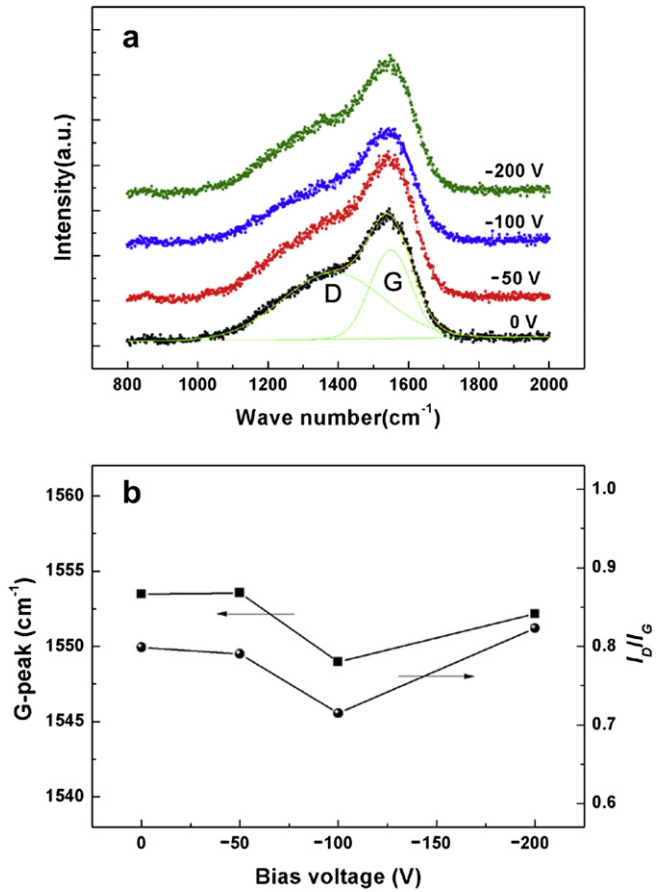


Fig. 5. (a) Typical Raman spectrum and Gaussian fitting, and (b) corresponding G-peak position and I_D/I_G of the films deposited at different bias voltage.

11 to 13 nm per minute. The high bias voltage would enhance the collisions of gas molecules and ions, and thus increased the plasma density, and cause the growth rate increase [15,16]. Furthermore, the bias voltage applied to the substrate could increase the ionized flux of metal and hydrocarbon radicals to the substrate. This also contributed to the growth rate increase [16].

The Cr/C atomic ratio of the films was measured by EDS and the results are presented in Fig. 3. The Cr concentration of the films significantly increased from 8.6 to 17 at% as the bias voltage increased from 0 to -200 V. The increase in chromium concentration may be attributed to the carbon re-sputtering caused by the high-energy ion bombardment. The weakly bonded carbon adatoms would be easily re-sputtered away by incident ions during the film growth stage [12,17].

The chemical bonds of the films deposited at the bias voltage of 0 and -100 V were analyzed by XPS and the corresponding high-resolution C 1s spectra are shown in Fig. 4. Both spectra have a major peak at a binding energy around 284.5 eV and a shoulder peak around 283 eV, the first of which could be assigned to C–C or C–H bonding and the second to Cr–C bonding respectively [7,18]. It should be noted that the intensity of the Cr–C peak around 283.0 eV showed a small increase as the bias voltage increased from 0 to -100 V, implying that the amount of the Cr–C bonding increased as the bias voltage increased. A weak peak was also observed at the binding energy of about 286 eV, corresponding to carbon in an oxide state. In fact, the broadening peak at 284.5 eV could be deconvoluted into two peaks with binding energies about 284.3 eV and 284.8 eV corresponding to sp^2 and sp^3 hybridized carbon bonding respectively [7,18]. However, it is very difficult to exactly separate the two peaks since they are so close.

More elaborate carbon bond analysis was performed by Raman spectroscopy, which is a popular, non-destructive tool to obtain the detailed bonding structure of the DLC films [9]. Fig. 5(a) presents the Raman spectra of the films deposited with various bias voltages. The DLC film Raman spectra can be fitted by two Gaussian peaks, D

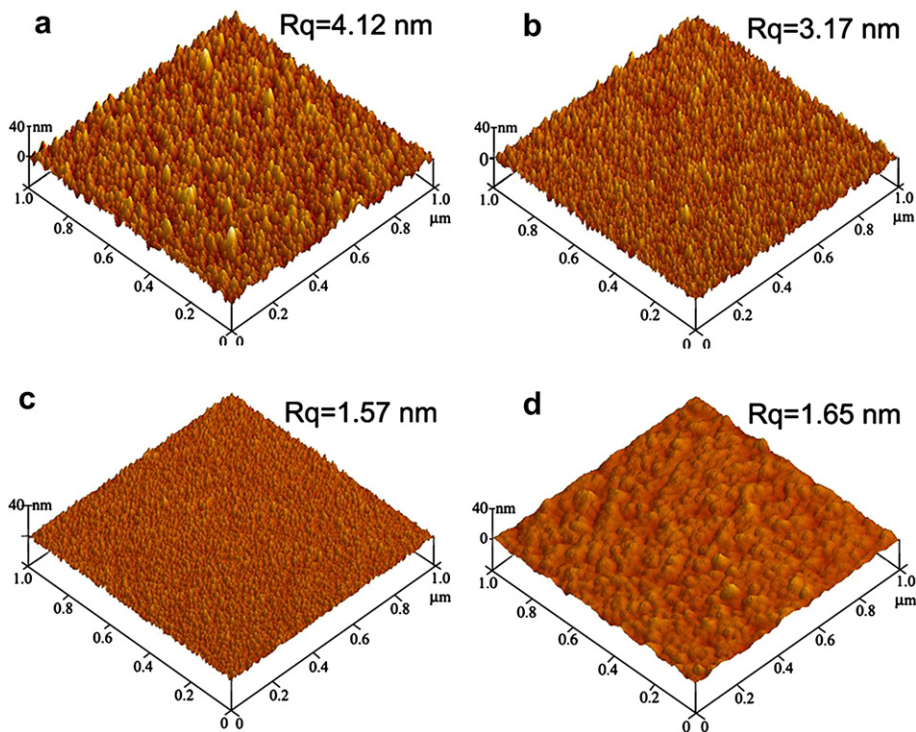


Fig. 6. AFM images of the films deposited at the bias voltage of (a) 0 V, (b) -50 V, (c) -100 V, and (d) -200 V.

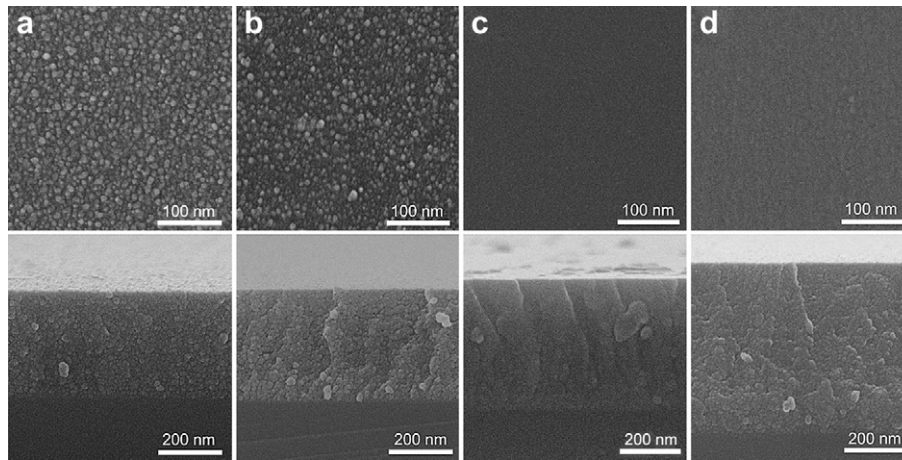


Fig. 7. Plan-view and cross-sectional SEM images of the films deposited at the bias voltage of (a) 0 V, (b) –50 V, (c) –100 V, and (d) –200 V.

peak (disorder) around 1350 cm^{-1} and G peak (graphite) around 1550 cm^{-1} [9]. The relative ratio of the D peak to G peak (I_D/I_G) and the position of G peak can be used to characterize the sp^3/sp^2 ratio [19]. Generally, the increase of the sp^3 bonding fraction will cause the G-peak position to shift down and the I_D/I_G ratio will decrease in hydrogenated DLC films [9,20]. The G-peak position and the ratio I_D/I_G as a function of the bias voltage are shown in Fig. 5(b). It should be noted that the position of the G-peak and the ratio I_D/I_G were decreasing with increasing bias voltage and then reached their lowest point at about –100 V. However, they increased subsequently when the bias voltage exceeded –100 V. This implied that the films had the maximum fraction of the sp^3 bonds at the bias voltage of about –100 V. The key process of the DLC deposition is the formation of sp^3 bonding. A “sub-plant” model by Robertson could be used to explain the relationship between the ion energy per C atom and sp^3 bonding fraction [9]. At low bias voltage, the ion energy is too low to penetrate into the growing surface, so the species would just stick to the growing surface and remain in its lowest energy state of sp^2 bonding. As the bias voltage increased to about –100 V, the ion species had sufficient energy to penetrate into the subsurface, and thus caused the local density increase, and promoted the sp^3 bonding formation. However, with the bias voltage increasing further, the ion energy exceeded the penetration threshold, and the excess energy would be dissipated as in other processes. This would cause the sp^3 fraction to decrease [9].

3.2. Surface morphology and roughness

The AFM micrographs of the films are given in Fig. 6. At the bias voltage of 0 V, the film showed dense high peaks on the surface. When the bias voltage increased up to –100 V, the film became flat and smooth, and the surface roughness decreased dramatically from 4.12 nm to 1.57 nm. Note however that the film deposited at the bias voltage of –200 V also showed a lower roughness of about 1.67 nm, although its surface consisted of some big agglomerates. Fig. 7 shows the plan-view and cross-sectional SEM images of the films deposited at different bias voltage. The images were in reasonable agreement with the AFM ones. Note that there were numerous hillocks on the surface of the film deposited at 0 V. As the bias voltage increased, the number of these hillocks decreased sharply, and the hillocks were absent when the bias voltage reached up to –100 V.

The ion bombardment effects were proposed to contribute to the surface smoothing process [12]. During the film growth, the Cr^+ and Ar^+ ions were attracted into the films and bombarded the

film surface. The effect of this ion bombardment would minimize the surface roughness of the films as the impinging ions would tend to transfer adatoms from the crest to the valley (as the AFM images showed) and smooth the film surface [8].

3.3. Wettability and mechanical properties

The wettability of the films was assessed using the water contact angle. Fig. 8 shows the contact angle of the films deposited with different bias voltage. The contact angle of the films was found to decrease when the bias voltage increased. Numerous previous studies have indicated that the surface features and roughness have a great influence on the surface wettability of the films [21–23]. As the bias voltage increased, the surface roughness of the films decreased, and this resulted in the decrease of the contact angles. Furthermore, the increase of metal concentration in the films due to the bias voltage increase was also expected to minimize the water contact angle [24].

Fig. 9(a) presents the hardness and elastic modulus of the films as a function of the bias voltage. The hardness and elastic modulus showed an increase as the bias voltage increased from 0 V to –50 V, and then reached a maximum value followed by a monotonic decrease with further increase of the bias voltage. The dependence of the film internal stress on the bias voltage is shown in Fig. 9(b). It is of note that the variation in the internal stress with bias voltage

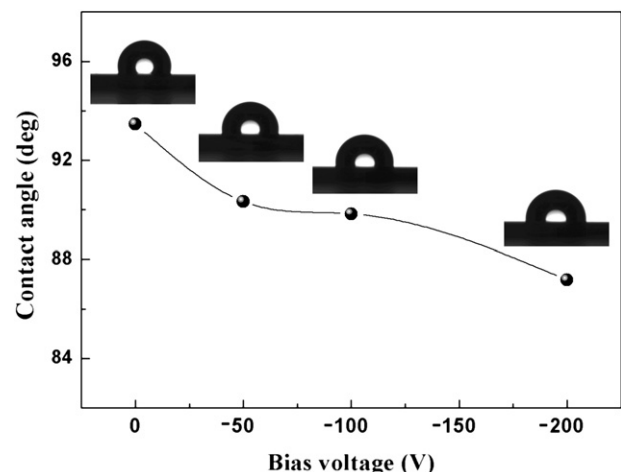


Fig. 8. Water contact angle of the films deposited at different bias voltage.

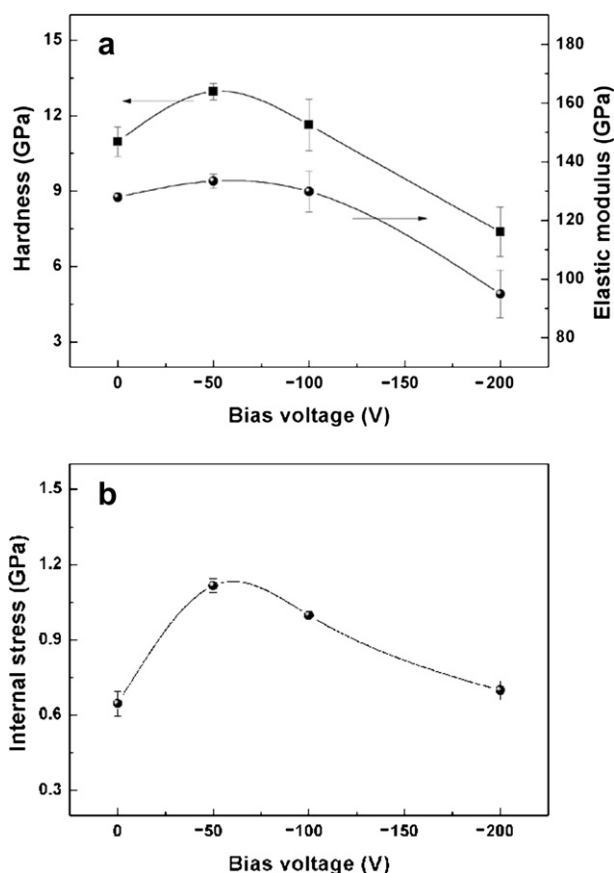


Fig. 9. (a) Hardness and elastic modulus, and (b) internal stress of the films as a function of bias voltage.

was similar to that of the hardness. Normally, both the mechanical properties and internal stress of the DLC films had a fairly proportional relationship with the sp^3 bond fraction [9]. However, according to the Raman analysis, the highest value of the sp^3 fraction was acquired at about -100 V. In fact, besides the sp^3 bonding fraction, there was another factor to be considered, the effect of Cr doping and ion bombardment, which may explain this phenomenon. On the one hand, the doping of chromium could break up the continuity of the carbon network, and thus cause the film hardness to decrease [7]. On other hand, the Cr^+ ion-assisted bombardment was expected to etch the weak bond and increase the film density, which would contribute to the increase of the hardness [25].

4. Conclusions

Cr-DLC films were deposited on silicon wafers by a co-deposition system comprising a linear ion source and a DC magnetron sputtering unit. The evolution of the film growth rate, chemical composition, atomic bonds, surface morphology, and mechanical properties were studied as a function of the bias voltage. The

growth rate and chromium concentration of the films increased monotonously with the bias voltage increase. However, the sp^3 bonding fraction exhibited the maximum value at the bias voltage of -100 V, and then it tended to decrease whether the bias voltage decreasing or increasing. The highest hardness and highest internal stress of the films were obtained at the bias voltage of -50 V. Besides the sp^3 bonding fraction, the effect of Cr doping and ion bombardment also had a significant influence on the mechanical properties of the films. With bias voltage increasing from 0 to -200 V, the surface topography of the films changed from a rough surface with large hillocks to a relatively smooth flat surface. As a result, the water contact angle decreased monotonously as the bias voltage increased. It is supposed that the bias voltage can be used to modify the surface morphology and mechanical property, and thus induce significant changes in the tribological characteristics, which have significant consequences in a broad range of applications.

Acknowledgements

The present research was financially supported by the project of Science and Technology Department of Zhejiang Province (Grant No: 2008C21055), the Natural Science Foundation (Grant No: 2007A610028) and International Cooperation Foundation (Grant No: 2008B10046) of Ningbo government, China.

References

- [1] Ding XZ, Tay BK, Lau SP, Zhang P, Zeng XT. *Thin Solid Films* 2002;408:183.
- [2] Pauleau Y, Thiery E. *Surf Coat Technol* 2004;180:313.
- [3] Schiffmann KI. *Surf Coat Technol* 2004;177:453.
- [4] Corbella C, Vives M, Pinyol A, Bertran E, Canal C, Polo MC, et al. *Surf Coat Technol* 2004;177–178:409.
- [5] Zhang S, Bui XL, Fu Y. *Thin Solid Films* 2004;467:261.
- [6] Wang AY, Lee KR, Ahn JP, Han JH. *Carbon* 2006;44:1826.
- [7] Singh V, Jiang JC, Meletis EI. *Thin Solid Films* 2005;489:150.
- [8] Pei YT, Chen CQ, Shaha KP, Hosson JThMDe, Bradley JW, Voronin SA, et al. *Acta Mater* 2008;56:696.
- [9] Robertson J. *Mater Sci Eng R* 2002;37:129.
- [10] Hovsepian PEh, Kok YN, Ehasarian AP, Erdemir A, Wen JG, Petrov I. *Thin Solid Films* 2004;447–448:7.
- [11] Kim D, Jang HS, Kim YS, Choi DH, Choi BK, Lee JH, et al. *Nucl Instrum Methods Phys Res Sect B* 2007;254:93.
- [12] Kok YN, Hovsepian PEh, Luo Q, Lewis DB, Wen JG, Petrov I. *Thin Solid Films* 2005;475:219.
- [13] Anders A. *Surf Coat Technol* 2005;200:1893.
- [14] Stoney GG. *Proc R Soc London Ser A* 1909;82:172.
- [15] Yin D, Xu N, Liu Z, Han Y, Zheng X. *Surf Coat Technol* 1996;78:31.
- [16] Zhang G, Yan P, Wang P, Chen Y, Zhang J, Wang L, et al. *Surf Coat Technol* 2008;202:2684.
- [17] Uglov VV, Kuleshov AK, Rusalsky DP, Samzov MP, Dementshenok AN. *Surf Coat Technol* 2002;158–159:699.
- [18] Wilson GM, Saied SO, Field SK. *Thin Solid Films* 2007;515:7820.
- [19] Casiraghi C, Ferrari AC, Robertson J. *Phys Rev B Condens Matter* 2005;72:085401.
- [20] Ferrari AC, Robertson J. *Phys Rev B Condens Matter* 2000;61:14095.
- [21] Zhou Y, Wang B, Song X, Li E, Li G, Zhao S, et al. *Appl Surf Sci* 2006;253:2690.
- [22] Zhou Y, Wang B, Zhang X, Zhao M, Li E, Yan H. *Colloids Surf A* 2009;335:128.
- [23] Paul R, Dalui S, Das SN, Bhar R, Pal AK. *Appl Surf Sci* 2008;255:1705.
- [24] Corbella C, Bertran E, Polo MC, Pascual E, Andujar JL. *Diamond Relat Mater* 2007;16:1828.
- [25] Wang DY, Weng KW, Chang CL, Guo XJ. *Diamond Relat Mater* 2000;9:831.